Title

PD-L1, TIM-3, and CTLA-4 Blockade Fails To Promote Resistance to Secondary Infection with Virulent Strains of Toxoplasma gondii

Journal

Infection and Immunity, 86(9)

ISSN

0019-9567

Authors

Splitt, Samantha D
Souza, Scott P
Valentine, Kristen M
et al.

Publication Date

2018-09-01

DOI

10.1128/iai.00459-18

Peer reviewed

AMERICAN SOCIETY FOR MICROBIOLOGY | Infection and Immunity®

MICROBIAL IMMUNITY AND VACCINES

PD-L1, TIM-3, and CTLA-4 Blockade Fails To Promote Resistance to Secondary Infection with Virulent Strains of *Toxoplasma gondii*

Samantha D. Splitt,[a] Scott P. Souza,[a] Kristen M. Valentine,[a] Brayan E. Castellanos,[a] Andrew B. Curd,[a] Katrina K. Hoyer,[a] Kirk D. C. Jensen[a]

[a]Molecular and Cell Biology Department, School of Natural Sciences, University of California, Merced, Merced, California, USA

ABSTRACT T cell exhaustion is a state of hyporesponsiveness that develops during many chronic infections and cancer. Neutralization of inhibitory receptors, or "checkpoint blockade," can reverse T cell exhaustion and lead to beneficial prognoses in experimental and clinical settings. Whether checkpoint blockade can resolve lethal acute infections is less understood but may be beneficial in vaccination protocols that fail to elicit sterilizing immunity. Since a fully protective vaccine for any human parasite has yet to be developed, we explored the efficacy of checkpoint inhibitors in a mouse model of *Toxoplasma gondii* reinfection. Mice chronically infected with an avirulent type III strain survive reinfection with the type I RH strain but not the MAS, GUY-DOS, and GT1 parasite strains. We report here that mouse susceptibility to secondary infection correlates with the initial parasite burden and that protection against the RH strain is dependent on CD8 but not CD4 T cells in this model. When given a lethal secondary infection, CD8 and CD4 T cells upregulate several coinhibitory receptors, including PD-1, TIM-3, 4-1bb, and CTLA-4. Moreover, the gamma interferon (IFN-γ) response of CD8 but not CD4 T cells is significantly reduced during secondary infection with virulent strains, suggesting that checkpoint blockade may reduce disease severity. However, single and combination therapies targeting TIM-3, CTLA-4, and/or PD-L1 failed to reverse susceptibility to secondary infection. These results suggest that additional host responses, which are refractory to checkpoint blockade, are likely required for immunity to this pathogen.

KEYWORDS atypical strains, CD4 T cells, CD8 T cells, CTLA-4, checkpoint blockade, PD-1, T cell exhaustion, TIM-3, *Toxoplasma gondii*, vaccine

T cell exhaustion is a state of cellular hyporesponsiveness that occurs in response to continued antigen stimulation or inflammation, wherein T cells produce fewer cytokines and cytotoxic molecules, lower expression levels of activating receptors, and increased expression levels of inhibitory receptors (1). T cell exhaustion was first characterized in chronic viral infection models (2–4) but is now widely studied in cancer (5–8), bacterial infection (9, 10), and parasitic infection models (11–13) and is in part a programmed response to limit immune pathology in these settings. The molecular signature of CD8 and CD4 T cell exhaustion has been thoroughly defined, and several markers have been identified to distinguish these hyporesponsive states (14–16). Several key markers that label CD8 or CD4 T cells as exhausted have been identified: (i) high expression levels of the inhibitory receptors PD-1, LAG-3, TIM-3, CTLA-4, 2B4, BTLA, and CD160; (ii) lowered expression levels of the costimulatory receptors 4-1bb, ICOS, and OX40; and (iii) differential expression of the transcription factors Tbet, Eomes, BLIMP-1, and others (17–19). Exhausted T cells may carry most, or a portion, of these markers, and marker expression varies with the disease model, severity of disease, and

Received 12 June 2018 **Accepted** 19 June 2018

Accepted manuscript posted online 2 July 2018

Citation Splitt SD, Souza SP, Valentine KM, Castellanos BE, Curd AB, Hoyer KK, Jensen KDC. 2018. PD-L1, TIM-3, and CTLA-4 blockade fails to promote resistance to secondary infection with virulent strains of *Toxoplasma gondii*. Infect Immun 86:e00459-18. https://doi.org/10.1128/IAI.00459-18.

Editor Judith A. Appleton, Cornell University

Address correspondence to Kirk D. C. Jensen, kjensen5@ucmerced.edu.

S.D.S. and S.P.S. contributed equally to this work.

cell type. Treatment with neutralizing antibodies that target inhibitory receptors, or "checkpoint blockade," has proven effective in reversing disease severity in a variety of mouse models for chronic viral infection and cancer (20, 21). Importantly, these observations have translated to high response rates, tumor regression, and even survival of late-stage melanoma patients (22–25). Therefore, checkpoint blockade is predicted to have a major impact on the treatment of human infectious disease (26, 27), but for which category of pathogen (bacterial, fungal, protozoan, helminth, or viral), which stage of infection (acute, chronic, or secondary), and which checkpoint blockade strategies should be used are less clear.

Toxoplasma gondii is a ubiquitous intracellular protozoan parasite that infects nearly all warm-blooded vertebrates and exhibits a great deal of genetic diversity, especially among "atypical" South American strains (28–31). *T. gondii* strains differ in virulence in mice, with type I and most atypical strains being virulent and type II and type III strains being relatively less virulent (32–35). By using these strains, the immune response to *T. gondii* can be examined under conditions of various infection intensities, a strategy that is commonly used to study T cell exhaustion in the lymphocytic choriomeningitis virus (LCMV) system. During the initial phase of infection, host control of *T. gondii* requires both innate and adaptive immune cells that make gamma interferon (IFN-γ) (36). Despite immune pressure, *T. gondii* rapidly disseminates to distal tissues (37) to chronically infect for the lifetime of the host. Both CD4 and CD8 T cells play pivotal roles in preventing reactivation of the chronic form of infection and in preventing toxoplasmic encephalitis (38–42). In this context, T cell exhaustion is a critical component of disease progression (43). Chronic infection with the intermediate-virulence type II ME49 strain will cause CD8 T cells to upregulate the inhibitory receptor PD-1 and exhibit diminished effector functions, including reduced IFN-γ and granzyme B (GzmB) production, in genetically susceptible C57BL/6 mice (13, 44). Bhadra et al. rescued exhausted CD8 T cells and parasite recrudescence following antibody blockade of PD-1 ligand (PD-L1) (13). They also observed a BLIMP-1-dependent CD4 T cell exhaustion program, with increased inhibitory receptor expression and decreased IFN-γ production during chronic *T. gondii* infection (45). These results underscore the importance of T cell exhaustion and the clinical potential of checkpoint inhibitors to resolve chronic infections, including *T. gondii* infection.

Can checkpoint blockade therapies be used to treat acute parasitic infections? In early studies on the scope and efficacy of anti-CTLA-4 therapy, it was clearly demonstrated to be beneficial in mouse models of acute visceral leishmaniasis (46) and hookworm infections (47). Furthermore, given the current difficulties in vaccine design for many parasitic pathogens, perhaps immunotherapy could be used as a second option to treat vaccinated individuals who fail to control parasitic infection. By correcting impaired memory T cell responses, immunotherapy could have a profound impact on such individuals. Importantly, immunotherapy would be blind to antigen, major histocompatibility complex (MHC) allele type, and vaccine regimen of the infected individual and could work on antibiotic-resistant parasites. In mouse models of *T. gondii* reinfection ("secondary infection" or "challenge"), vaccinated (48–51) or chronically infected (52) mice are not susceptible to secondary infections with the highly virulent type I RH strain. Although naive mice fail to control infection with as few as one parasite of the type I strain, adoptive transfer of memory CD8 T cells to naive mice confers protection (50, 53). While primary infection with vaccine or avirulent *T. gondii* strains can induce protective immunity to many virulent *T. gondii* strains, this is not true for most atypical strains (52).

Here we hypothesized that susceptibility of C57BL/6 mice to secondary infection may be due to dysfunctional T cell responses caused by highly virulent *T. gondii* strains. Moreover, we tested whether neutralization of inhibitory receptors that promote T cell dysfunction could induce mouse survival following secondary infection. Although CD8 T cells expressed exhaustion markers and exhibited diminished IFN-γ responses during secondary infection with virulent *T. gondii* strains, mice were not protected from

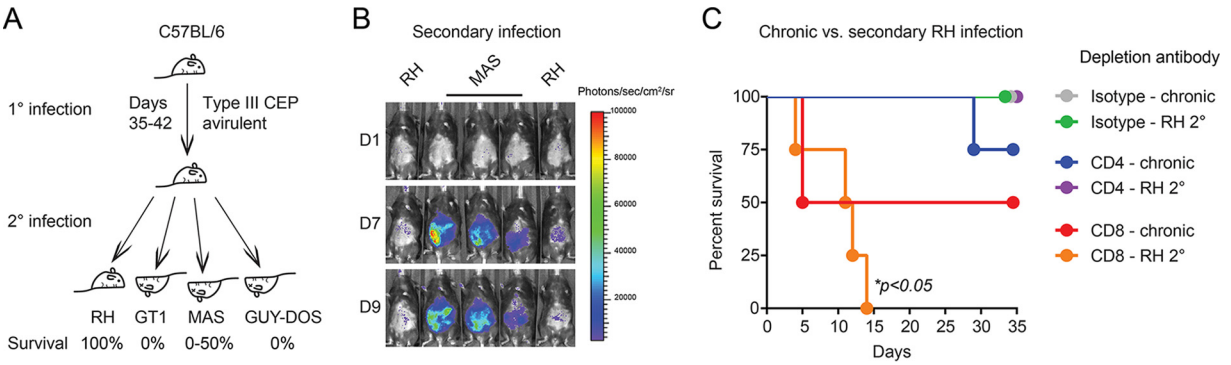

FIG 1 Requirement for CD8 T cells in a mouse model of *T. gondii* secondary infection. (A) Schematic of the model used to assess T cell exhaustion during secondary infection with virulent strains that cause lethal (MAS, GUY-DOS, and GT1) and nonlethal (RH) outcomes. Average percent survivals from previous results (52) are indicated. (B) Representative bioluminescence imaging of individual C57BL/6 mice following secondary infection with the RH (1-1) and MAS (2C8) luciferase-expressing strains. Relative parasite burdens are depicted as a heat map, and the maximum and minimum values were set to 10^5 and 3×10^3 photons/s/cm^2/sr, respectively. (C) Following chronic infection, mice were treated with depletion antibodies to either CD8 or CD4 or given an isotype control antibody for 1 week and then challenged with RH (RH 2°) or not challenged (chronic). The depletion regimen was continued until day 11. Cumulative survival rates from two separate experiments are plotted ($n = 4$ mice per group); *P* values were obtained by using the log rank Mantel-Cox test comparing depleted cohorts against similarly infected isotype control-treated groups ($n = 2$ mice per isotype-treated group).

challenge with the atypical strain MAS or the type I GT1 strain when administered neutralization antibodies to CTLA-4, TIM-3, and/or PD-L1.

RESULTS

To explore the role of T cell exhaustion during acute secondary infections with *T. gondii*, genetically susceptible C57BL/6 mice were first injected intraperitoneally (i.p.) with the avirulent type III CEP *hxgprt*$^-$ strain, which forms a nonlethal chronic infection, and 35 to 45 days later, mice were then reinfected (i.e., "secondary infection" or "challenge") with either the atypical strains MAS and GUY-DOS or the highly passaged laboratory type I strain RH (Fig. 1A). All three *T. gondii* strains cause a lethal primary infection in naive mice (34, 35, 52); however, chronically infected C57BL/6 mice survive secondary infection with RH but not the MAS or GUY-DOS strain (52). In this model, susceptibility to secondary infection correlates with increased parasite numbers, which can be observed by bioluminescence imaging of mice between days 5 and 12 of secondary infection with luciferase-expressing MAS compared to the RH strain (Fig. 1B and data not shown). Consistent with cellular requirements for immunity reported in vaccination studies (48–50), depletion of CD8 but not CD4 T cells after primary infection abrogated protection against RH challenge (Fig. 1C). Moreover, depletion of CD8 but not CD4 T cells impaired the ability of mice to control chronic infection. Both lineages of T cells are required to prevent reactivation in mice chronically infected with an intermediate-virulence type II strain, ME49 (39, 54), and CD8 T cells are the primary effector T (T_E) cells responsible for cyst removal in this setting (41, 55). Overall, our model, which uses an avirulent type III strain to generate immunological memory, is consistent with the above-mentioned models for chronic infection- and vaccine-induced immunity and positions memory CD8 T cells as central players in host resistance to *T. gondii*.

The T cell populations analyzed for exhaustion makers were defined by the expression of CD62L (L-selectin) and KLRG1 (killer cell lectin-like receptor G1). CD62L is a cell adhesion molecule important for homing lymphocytes into the T cell zone of secondary lymphoid tissues and is expressed on naive T cells and central memory T (T_{CM}) cells (56). In response to T cell receptor (TCR) triggering by antigen, T_{CM} cells initially produce a very minimal repertoire of cytokines, namely, interleukin-2 (IL-2), but following differentiation into effector T cells, these cells also produce large amounts of cytokines and granzyme (57). Effector memory T (T_{EM}) cells are active, cytokine-producing cells that, like T_E cells, do not express CD62L; instead, they express inflammatory chemokine

receptors that home these cells to the site of infection. KLRG1 is a transmembrane protein found on lymphocytes that marks highly activated, terminally differentiated T_E and T_{EM} cells following microbial infections, including *T. gondii* infection (58–60). CD8 T cells expressing CD62L or KLRG1 have different requirements for IL-12 during differentiation and different abilities to make IFN-γ during *T. gondii* infection (59, 61). Using this staining approach, the percentages (Fig. 2A and B) and numbers (Fig. 2C) of CD62L$^+$ KLRG1$^-$ ("CD62L$^+$"), CD62L$^-$ KLRG1$^-$, and CD62L$^-$ KLRG1$^+$ ("KLRG1$^+$") CD8 T cells isolated from the peritoneal cavity significantly increased following chronic infection compared to those in naive animals. On day 5 of secondary infection with either the type I RH strain or the atypical strains MAS and GUY-DOS, the relative percentages and cell numbers of each population remained constant compared to those during chronic infection. A similar trend was also observed for CD4 T cell populations in the peritoneum (Fig. 2). Changes in splenic T cell responses were found to be minimal in this system, as discussed below. Thus, peritoneal T_E- or T_{EM}-like T cells expand at the site of initial infection, and their level of cellularity remains high following challenge.

Cell surface expression levels of several inhibitory receptors and one costimulatory receptor associated with T cell exhaustion in the LCMV model (14, 16), PD-1, TIM-3, CTLA-4, and 4-1bb, respectively, were measured on the various CD8 T cell populations described in the legend of Fig. 2. Compared to CD8 T cells from chronically infected mice or mice challenged with RH, CD8 T cells from mice challenged with the atypical strains MAS and GUY-DOS exhibited increased expression levels of PD-1 and TIM-3, most noticeably on the CD62L$^-$ KLRG1$^-$ and KLRG1$^+$ (T_{EM}-like) populations (Fig. 3A and B). The costimulatory tumor necrosis factor (TNF) superfamily receptor 4-1bb also showed modest but significantly increased expression on CD62L$^-$ KLRG1$^{+/-}$ CD8 T cell populations following virulent compared to nonvirulent secondary or chronic infections. The NK cell receptor 2B4, associated with T cell survival during secondary LCMV infections (62), was upregulated on CD62L$^-$ KLRG1$^{+/-}$ CD8 T cell populations following chronic infection compared to those in naive mice but was not upregulated in response to virulent secondary infections with the MAS strain (not shown). Because CTLA-4 expression was only marginally detected on the surface of CD8 T cells in this model (not shown), likely due to rapid internalization following T cell activation (63), intracellular staining was implemented. Increased CTLA-4 protein expression was observed in CD8 T cells following lethal secondary compared to nonlethal infections; however, statistical significance was not reached due to individual mouse variability. Finally, because the degree of CD8 T cell hyporesponsiveness correlates with the coexpression of multiple inhibitory receptors (64), the frequency of CD8 T cell populations that coexpress PD-1 and TIM-3 or PD-1 and CTLA-4 was determined. Compared to nonlethal conditions, secondary infections with virulent strains significantly enhanced the coexpression of PD-1 and TIM-3 on each CD8 T cell population analyzed (Fig. 3C and D). The coexpression of CTLA-4 and PD-1 also followed a similar trend; however, statistical significance between lethal and nonlethal infections was achieved only for CD62L$^+$ CD8 T cells, likely reflecting individual mouse variability in CTLA-4 expression. In summary, the expression of several T cell exhaustion markers, PD-1, TIM-3, 4-1bb, and, to a lesser extent, CTLA-4, on peritoneal CD8 T cells correlates with host susceptibility to secondary infection with *T. gondii*.

The same exhaustion marker profile was evaluated for CD4 T cells in the peritoneum (Fig. 4). Like CD8 T cells, CD4 T cells exhibited increased expression levels of PD-1, TIM-3, and 4-1bb (data not shown) in response to lethal secondary compared to nonlethal infections (Fig. 4A and B). Subtle differences were noted between CD4 and CD8 T cells, in which higher frequencies of PD-1 but lower frequencies of TIM-3 were observed for KLRG1$^+$ CD4 T cells than for their CD8 T cell counterparts. The level of CTLA-4, an inhibitory receptor highly expressed on CD4 T cells during exhaustion in the LCMV model (16), was also elevated in response to lethal challenge, but statistical significance was not obtained due to individual mouse variation. Because CTLA-4 is constitutively expressed on regulatory T cells (65), the frequency and contribution of these cells to the overall CTLA-4 signal in CD4 T cells were quantified (Fig. 4C and D). The frequency of

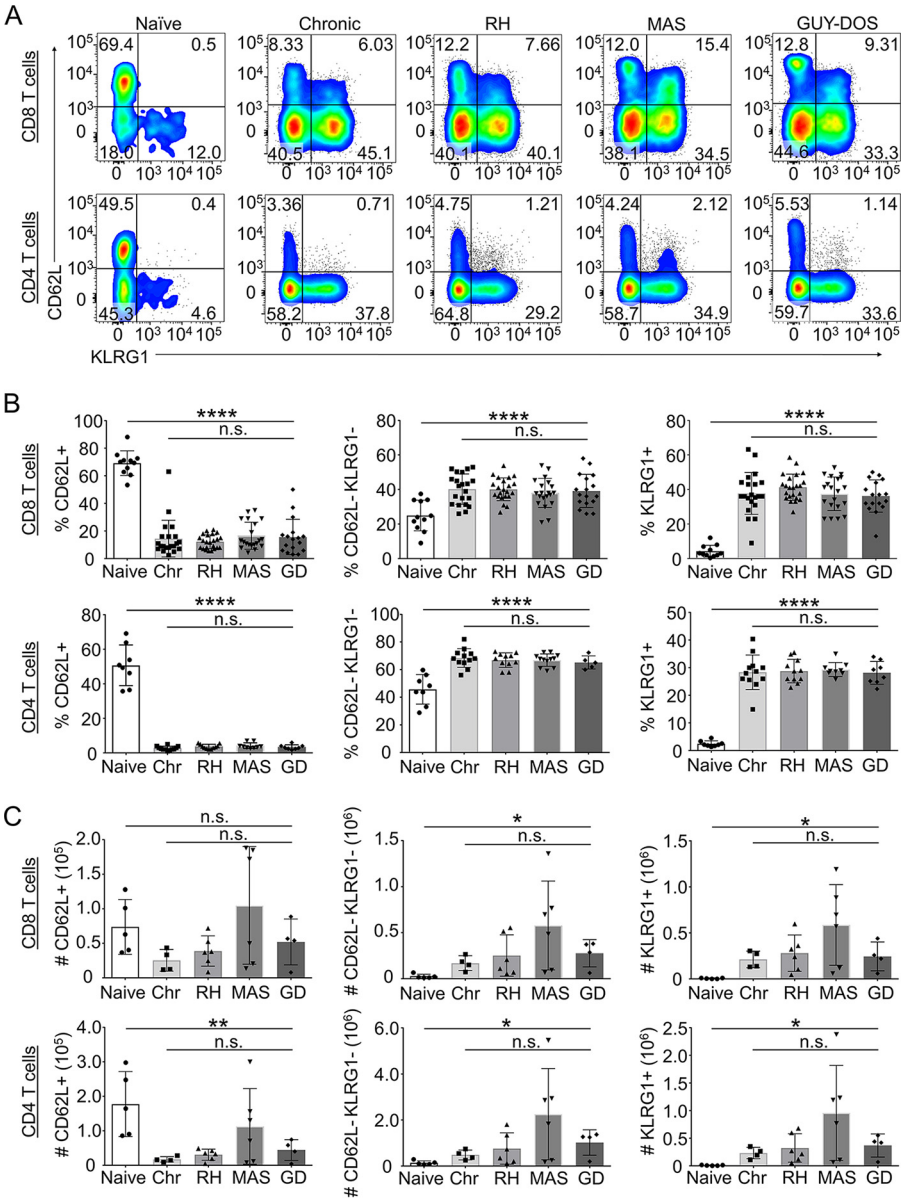

FIG 2 Frequencies of effector T cell populations following chronic and secondary infections with various *T. gondii* strains. (A) Representative flow plots of $CD8^+$ and $CD4^+$ ($CD3^+$ $CD19^-$) peritoneal T cells and their expression of CD62L and KLRG1 from naive C57BL/6 mice, mice that were infected with the type III CEP *hxgprt*$^-$ strain and allowed to progress to chronic infection for 35 to 45 days (Chronic), or chronically infected mice that were challenged with the indicated *T. gondii* strains and analyzed on day 5 of secondary infection. Numbers are the frequencies of cells that fall within the indicated gate. (B) Average frequencies ± standard deviations (SD) of the indicated cell populations, $CD62L^+$ $KLRG1^-$ ($CD62L^+$), $CD62L^-$ $KLRG1^-$, or $CD62L^-$ $KLRG1^+$ ($KLRG1^+$), among total $CD4^+$ or $CD8^+$ ($CD3^+$ $CD19^-$) T cells. Each dot represents the data from one mouse, and cumulative results from three to five experiments for CD4 T cell analysis and from six to eight experiments for CD8 T cell analysis are shown. (C) Same as for panel B, except that absolute cell numbers in the peritoneum were inferred from fluorescent bead recovery after peritoneal wash and counting by FACS analysis. Cumulative results from two separate experiments are plotted. *P* values were calculated with one-way ANOVA. n.s., nonsignificant; *, $P < 0.05$; **, $P < 0.01$; ****, $P < 0.0001$. The top bar compares the means for all groups; the bottom bar compares the means for all infected mice of the following groups: chronic (Chr), RH, MAS, and GUY-DOS (GD).

$FOXP3^+$ $CD25^+$ cells among total CD4 T cells dropped from 5.9% in naive mice to 1% following chronic infection or challenge. Although 97 to 100% of $FOXP3^+$ $CD25^+$ peritoneal CD4 T cells are CTLA-4^+ (not shown), these cells represent 5% of the total CTLA-4 signal among CD4 T cells following *T. gondii* secondary infection (Fig. 4D).

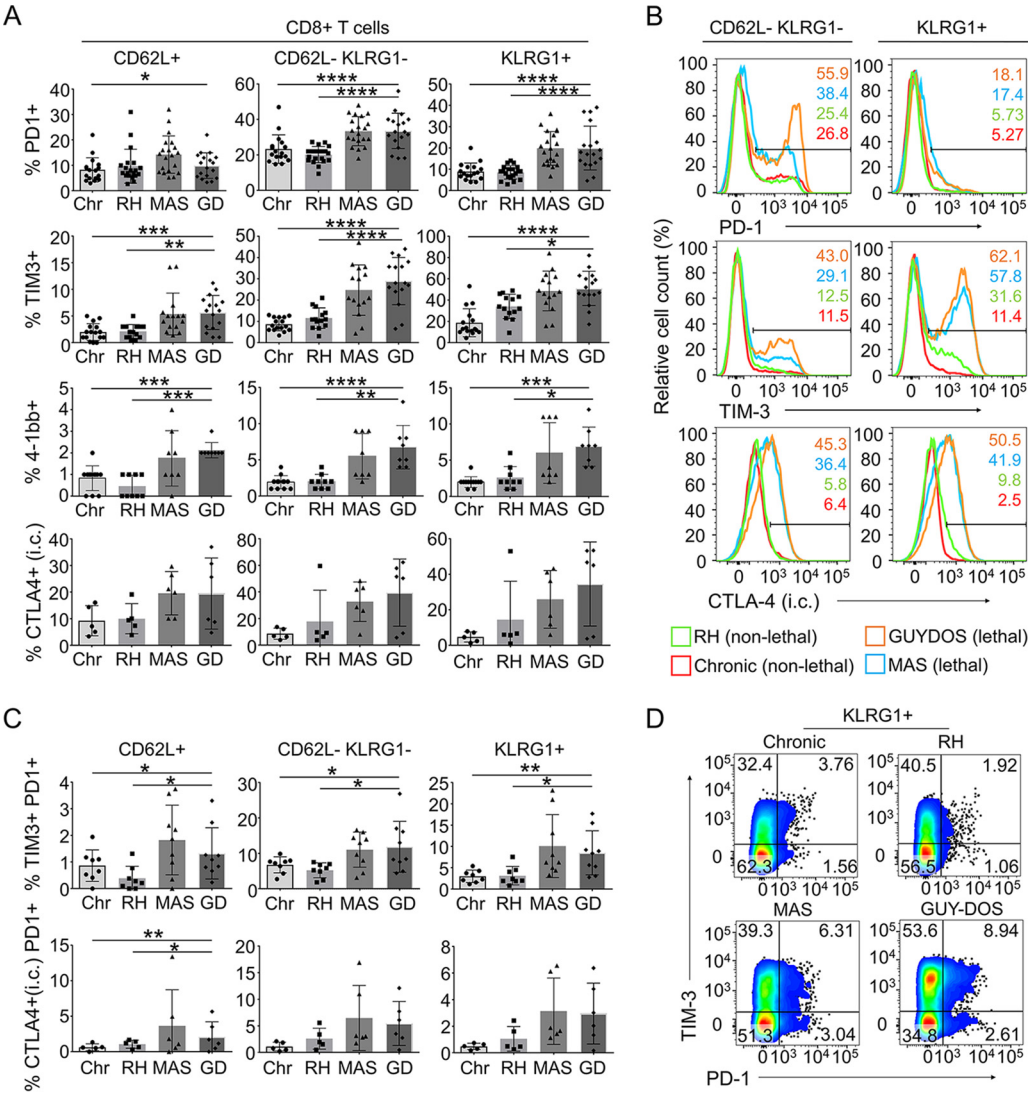

FIG 3 Markers of T cell exhaustion are highly expressed on CD8 T cells following secondary infection with virulent strains of *T. gondii*. (A) Average frequencies ± SD of CD62L$^+$ KLRG1$^-$ (CD62L$^+$), CD62L$^-$ KLRG1$^-$, or CD62L$^-$ KLRG1$^+$ (KLRG1$^+$) CD8$^+$ (CD3$^+$ CD19$^-$) peritoneal T cells that express the indicated exhaustion markers. Each dot represents data from one mouse on day 5 of secondary infection with RH, MAS, and GUY-DOS (GD) or without challenge (chronic infection [Chr]); cumulative results from three to seven experiments for PD-1, TIM-3, and 4-1bb and from two experiments for CTLA-4 are plotted. Significant *P* values (one-way ANOVA) are indicated for the means for all infected mice or mice given a secondary infection. *, $P < 0.05$; **, $P < 0.01$; ***, $P < 0.001$; ****, $P < 0.0001$. (B) Representative histogram plots of surface PD-1, TIM-3, or intracellular (i.c.) CTLA-4 expression for peritoneal CD62L$^-$ KLRG1$^-$ or KLRG1$^+$ CD8$^+$ T cells. Numbers represent the frequencies of cells that fall within the indicated gate; numbers and histogram lines are color-coded to match the indicated *T. gondii* infections. (C) Same as for panel A, except that the average frequencies ± SD of PD-1- and TIM-3- or CTLA-4 (i.c.)-coexpressing cells among the indicated CD8 T cell populations is plotted. Cumulative results from two to three experiments are shown. (D) Representative flow plots of peritoneal KLRG1$^+$ CD8$^+$ T cells for the expression of TIM-3 and PD-1. Numbers represent the frequencies of cells that fall within the indicated gates.

Therefore, effector CD4 T cells represent the majority of CTLA-4-expressing cells in the peritoneum following *T. gondii* infection. Finally, PD-1 expression correlated significantly with TIM-3 on all CD4 T cell populations analyzed and with CTLA-4 among KLRG1$^+$ CD4 T cells following lethal compared to nonlethal infections (Fig. 4E and F). In summary, the expression of T cell exhaustion markers on peritoneal CD4 T cells also correlates with host susceptibility to secondary infection, thus representing a shared characteristic of both T cell lineages in response to virulent challenge with *T. gondii*.

To assess whether increased expression of exhaustion markers on T cells correlated with a diminished capacity to produce IFN-γ, the critical cytokine required for immunity

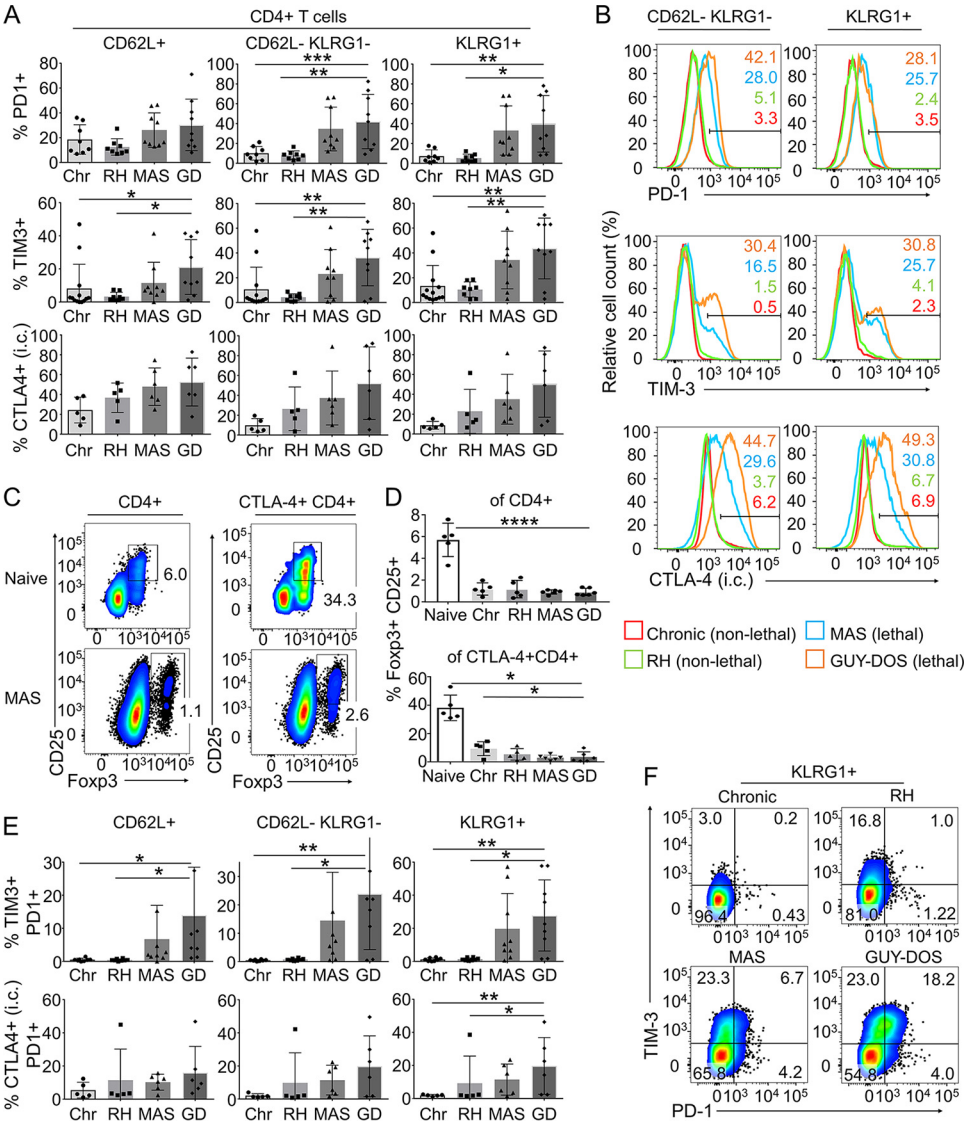

FIG 4 Markers of T cell exhaustion are upregulated on CD4 T cells following secondary infection with virulent strains of *T. gondii*. (A) Average frequencies ± SD of CD62L$^+$ KLRG1$^-$ (CD62L$^+$), CD62L$^-$ KLRG1$^-$, or CD62L$^-$ KLRG1$^+$ (KLRG1$^+$) CD4$^+$ (CD3$^+$ CD19$^-$) peritoneal T cells that express the indicated exhaustion marker. Each dot represents data from one mouse on day 5 of secondary infection with RH, MAS, and GUY-DOS (GD) or without challenge (chronic infection [Chr]), and cumulative results from three to four experiments are plotted. Significant *P* values (one-way ANOVA) are indicated for the means for all infected mice or mice given a secondary infection. *, $P < 0.05$; **, $P < 0.01$; ***, $P < 0.001$; ****, $P < 0.0001$. (B) Representative histogram plots of PD-1, TIM-3, and intracellular (i.c.) CTLA-4 expression for peritoneal CD62L$^-$ KLRG1$^-$ or KLRG1$^+$ CD4$^+$ T cells. Numbers represent the frequencies of cells that fall within the indicated gate; numbers and histogram lines are color-coded to match the indicated *T. gondii* infections. (C) Representative flow plots depicting CD25$^+$ and FOXP3$^+$ (i.c.) staining of total CD4$^+$ or CTLA-4$^+$ CD4$^+$ T cells from naive mice or from mice on day 5 of secondary infection with the MAS strain. Frequencies of cells that fall within the gates are shown. (D) Average frequencies ± SD of FOXP3$^+$ CD25$^+$ cells among total CD4$^+$ T cells (top) or total CTLA4$^+$ CD4$^+$ T cells (bottom). Statistical analysis was performed as described above for panel A, and cumulative results are plotted from two experiments. (E) Same as for panel A, except that the average frequencies ± SD of PD-1- and TIM-3- or CTLA-4 (i.c.)-coexpressing cells among the indicated CD4$^+$ T cell populations are plotted. Cumulative results from two to three experiments are shown. (F) Representative flow plots of peritoneal KLRG1$^+$ CD4$^+$ T cells for the expression of TIM-3 and PD-1. Frequencies of cells that fall within the gates are indicated.

to *T. gondii* (43), its expression was measured by *in vitro* recall and intracellular flow analyses. Peritoneal exudate cells (PECs) were harvested from chronically infected C57BL/6 mice or from mice on day 5 of secondary infection with the various parasite strains. PECs were then infected with *T. gondii in vitro* ("recall") and evaluated 16 h later for intracellular IFN-γ expression (52, 59). Relative to challenge with the RH strain, CD8

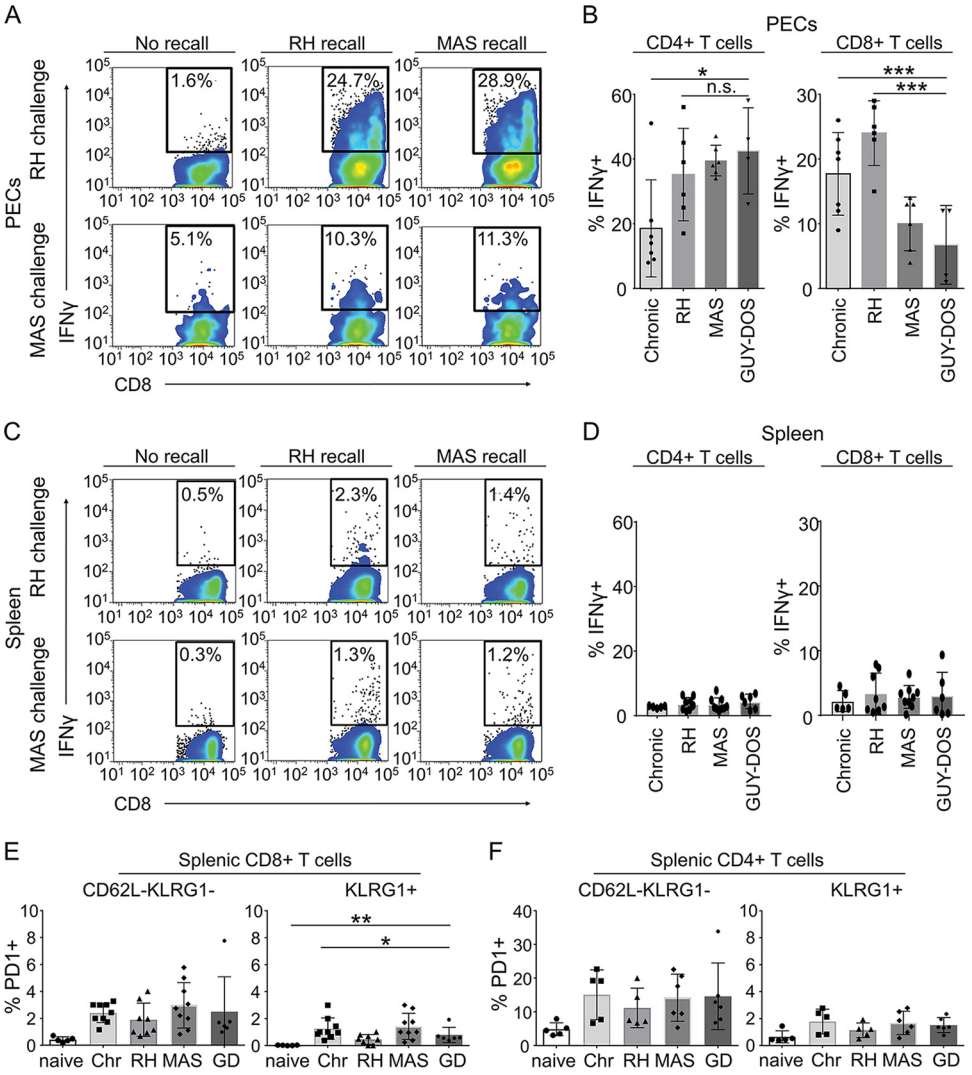

FIG 5 CD8 T cells produce less IFN-γ following challenge with virulent strains of *T. gondii*, while CD4 T cells are unimpaired. (A) PECs harvested from C57BL/6 mice on day 5 of secondary infection with the indicated *T. gondii* strains were infected *in vitro* ("recalled") with either the RH or MAS strain or not infected *in vitro* ("no recall"), and 16 h later, intracellular staining for IFN-γ and flow analysis were performed. Representative flow plots depicting the frequencies of $CD8^+$ ($CD3^+$ $CD19^-$) T cells that stain positive for IFN-γ within the indicated gate are shown. The IFN-γ response was independent of the strain type used in the *in vitro* recall assay (not shown for GUY-DOS). (B) Average frequencies ± SD of IFN-γ^+ $CD4^+$ or IFN-γ^+ $CD8^+$ ($CD3^+$ $CD19^-$) peritoneal T cells from chronically infected mice or from mice challenged with the indicated parasite strains. Each dot represents the data from one mouse following *in vitro* recall with the RH strain, and cumulative data from one (GUY-DOS) to three experiments (all other infections) are plotted. *, $P < 0.05$; **, $P < 0.01$; ***, $P < 0.001$; n.s., nonsignificant (one-way ANOVA). (C) $CD8^+$ T cells from the spleen were analyzed for IFN-γ expression from the same mice as for panel A. (D) Same as for panel B, except that the average frequencies ± SD of IFN-γ^+ $CD4^+$ or IFN-γ^+ $CD8^+$ ($CD3^+$ $CD19^-$) splenic T cells are shown. Cumulative data from two to three experiments are shown. (E and F) Average frequencies of PD-1^+ $CD62L^-$ $KLRG1^-$ or $CD62L^-$ $KLRG1^+$ ($KLRG1^+$) $CD8^+$ ($CD3^+$ $CD19^-$) (E) or $CD4^+$ (F) T cell populations. Each dot represents results from individual naive mice, chronically infected (Chr) mice, or mice challenged with RH, MAS, or GUY-DOS (GD) on day 5 of secondary infection. Cumulative results from two to three experiments are plotted, and statistics were calculated as described above for panel B.

T cells from mice challenged with atypical strains displayed a diminished capacity to produce IFN-γ (Fig. 5A and B). The recall IFN-γ response was independent of the parasite strain used for the *in vitro* recall infection (RH, MAS, or GUY-DOS) (Fig. 5A and data not shown). In contrast to CD8 T cells, and despite expressing exhaustion markers (Fig. 4), CD4 T cell IFN-γ production was not impaired but rather increased following secondary infection, and this response was irrespective of the parasite strain used for secondary infection (Fig. 5B). In the spleen, very minimal IFN-γ responses (Fig. 5C and

D) or exhaustion marker profile differences for PD-1, TIM-3, or CTLA-4 were observed for splenic T cells following RH, MAS, and GUY-DOS secondary infections (Fig. 5E and F and data not shown). Compared to peritoneal CD8 T cells from animals vaccinated with a replication-deficient type I RH strain, splenic CD8 T cell IFN-γ responses are known to be greatly reduced after challenge (50). Lowered splenic T cell responses may therefore represent a general feature following i.p. priming with less-virulent *T. gondii* strains, as observed previously (52).

PD-1—PD-L1 neutralization proved effective in promoting mouse survival during chronic infection with the intermediate-virulence type II ME49 *T. gondii* strain (13) but has not been tested during secondary challenge with virulent *T. gondii* strains. To test whether disease outcomes could be reversed following virulent challenge, several neutralizing antibodies were administered to block the pathways of inhibitory receptors most highly expressed on T cells in this system. Both the atypical strain MAS and the type I GT1 strain were used to understand the therapeutic efficacies of the various checkpoint blockade strategies. Like MAS and GUY-DOS, the GT1 strain also induces a lethal secondary infection in C57BL/6 mice (52) and induces the expression of PD-1 on CD62L$^-$ T_{EM}-like CD8 T cells (Fig. 6E). Although the expression level of the PD-1 ligand PD-L1 was not directly measured, treatment with neutralizing antibodies against PD-L1 is routinely used to block PD-1—PD-L1 signaling (18, 20). PD-L1 blockade failed to rescue mice following challenge with the atypical strain MAS (Fig. 6A), which exhibited similar parasite burdens between treated and control cohorts (Fig. 6B and C), and failed to rescue mice challenged with the GT1 strain (Fig. 6D). Combining PD-L1 blockade with anti-TIM-3 neutralizing antibodies promotes favorable disease outcomes in chronic LCMV infection (66) and in tumor models (7). However, neither TIM-3 blockade nor combination therapy with PD-L1 rescued mice following challenge with GT1 (Fig. 6D).

CTLA-4 attenuates T cell proliferation through competition for B7-1/2 ligands with the costimulatory receptor CD28 (67, 68) and by the recruitment of the PP2A phosphatase to the TCR-proximal signaling cascade, thereby deactivating Akt (69). CTLA-4 blockade is known to increase CD4 T cell IFN-γ responses in cancer patients (70). Moreover, since CTLA-4 neutralization converts memory CD8 T cells to effector T cells through Treg–CTLA-4-mediated suppression (71), and *ctla4*$^{-/-}$ transgenic CD8 T cells demonstrated enhanced secondary but not primary proliferative responses to antigen stimulation (72), the role of CTLA-4 blockade was explored in this system. However, neither a single CTLA-4 blockade nor combination therapy with PD-L1 altered survival following challenge with either strain (Fig. 6A and D). The capacity of peritoneal CD4 and CD8 T cells to produce IFN-γ, IL-2, and GzmB in the context of anti-PD-L1–anti-CTLA-4 combination therapy was explored. Following MAS challenge, modest but borderline significant (by chi-squared tests [Fig. 6G] and *t* tests [not shown]) increases in the frequencies of T cells that produce two or three of the measured immune mediators were observed for the treated compared to control cohorts (Fig. 6F and G). Resistance to checkpoint blockade is known to be caused by systemic IFN-γ signaling (73, 74). Since IFN-γ is highly produced by many cell types and detected in the serum following secondary infection (data not shown), the sustained presence of IFN-γ may cause the minimal T cell reinvigoration observed in this system. Regardless, these results suggest that blockade of the inhibitory pathways studied here, which are commonly targeted to reverse disease outcomes in mouse models of cancer, LCMV, and chronic *T. gondii* infections, is not suitable to treat acute secondary infections with virulent *T. gondii* strains.

DISCUSSION

The immune evasion mechanisms used by human parasitic pathogens, including *T. gondii*, are abundant and have contributed to the difficulty of parasitic disease prevention. Today, only one vaccine exists for any human parasitic pathogen, *Plasmodium falciparum*, and its efficacy is very low (25% efficacy; RTS,S) (75). Most vaccines fail to elicit long-lasting effector T cell responses (76), which are required to kill many parasitic pathogens (77, 78). Given the challenges with parasite vaccination and the estimated

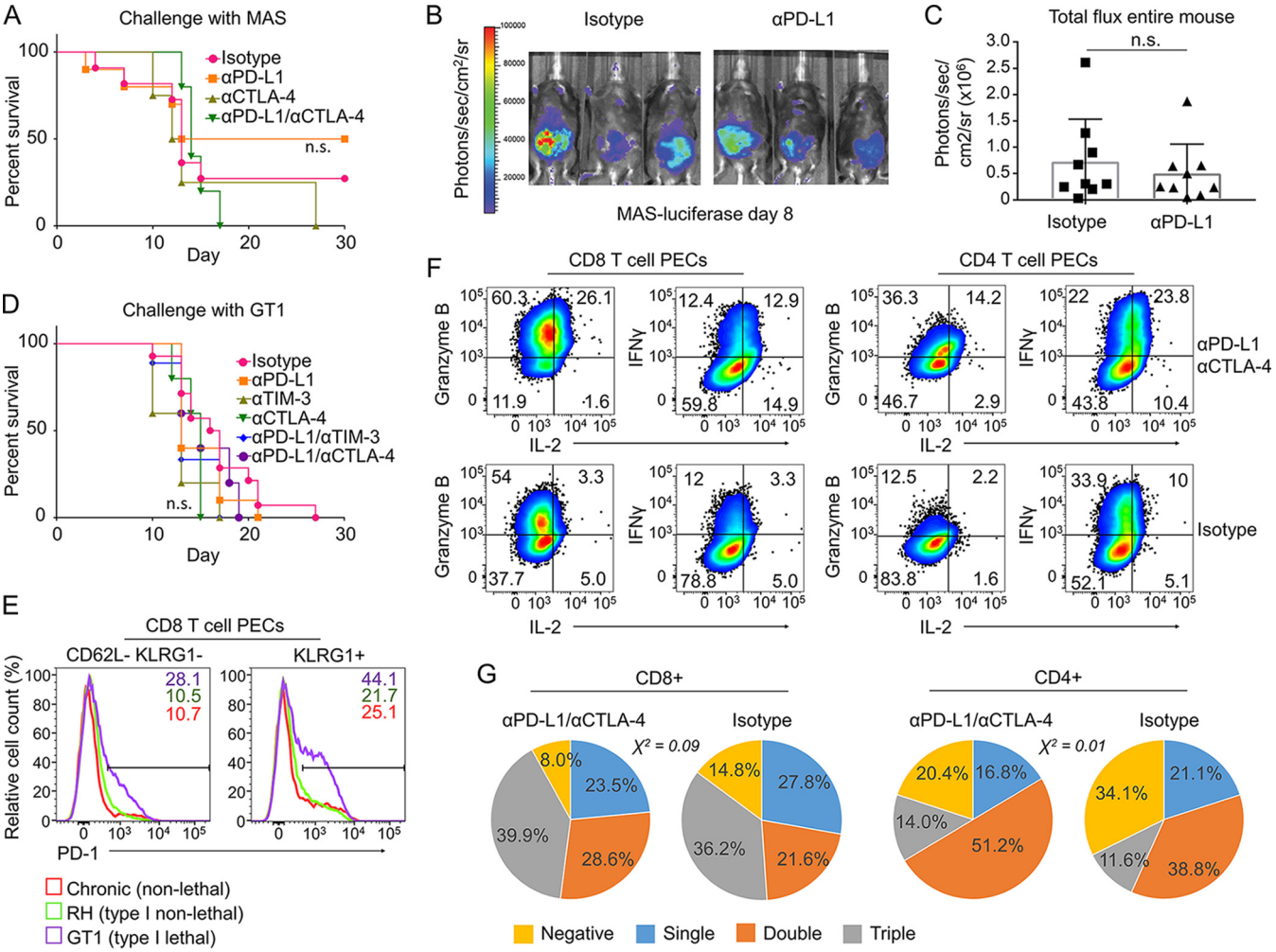

FIG 6 Neutralization with CTLA-4-, TIM-3-, and/or PD-L1-blocking antibodies fails to rescue C57BL/6 mice following challenge with virulent *T. gondii* strains. (A and D) Following secondary infection with either the virulent atypical strain MAS (A) or the type I strain GT1 (D), mice were injected i.p. with 200 μg of the following monoclonal antibodies on days 1, 3, 5, 7, 10, and 13 after challenge, and cumulative survival rates from one to two experiments are plotted: rat IgG2b isotype (GT1, $n = 9$; MAS, $n = 11$), anti-PD-L1 (GT1, $n = 9$; MAS, $n = 10$), anti-TIM-3 (GT1, $n = 5$), anti-CTLA-4 (GT1, $n = 5$; MAS, $n = 4$), anti-PD-L1 plus anti-TIM-3 (GT1, $n = 9$), and anti-PD-L1 plus anti-CTLA-4 (GT1, $n = 5$; MAS, $n = 5$). *P* values (log rank Mantel-Cox test) were calculated by comparing each therapeutic cohort against the control arm (isotype treated); all *P* values were >0.05 and considered not significant (n.s.). (B) Representative bioluminescence images of mice treated with anti-PD-L1 or the rat IgG2b isotype control on day 8 of secondary infection with the MAS-luciferase strain. (C) Same as for panel B, except that the average total body photon emissions (photons per second per square centimeter per steradian) ± SD are plotted. Each dot represents the measurement for an individual mouse, and cumulative data from two experiments are shown. The *P* value was >0.05 (one-way ANOVA), which was not significant. (E) Representative histogram plots from three separate experiments ($n = 3$ to 5 mice per experiment) of PD-1 expression on CD62L$^-$ KLRG1$^-$ or CD62L$^-$ KLRG1$^+$ (KLRG1$^+$) CD8$^+$ (CD3$^+$ CD19$^-$) peritoneal T cells during chronic infection or on day 5 of secondary infection with the type I RH or GT1 strain. Numbers represent the frequencies of cells that fall within the indicated gates and are color-coded to match the indicated *T. gondii* infections. (F) Representative flow plots of peritoneal CD8$^+$ and CD4$^+$ (CD3$^+$ CD19$^-$) T cells from mice treated with PD-L1 plus anti-CTLA-4 or with the isotype control on day 8 of secondary infection with the MAS strain. Intracellular detection of IFN-γ, IL-2, and GzmB was performed after *in vitro* recall infection, as described in the legend of Fig. 5; frequencies of cells that fall within each quadrant are shown. (G) Same as for panel F, except that the average frequencies of CD8 or CD4 T cells that express all three (triple), at least two (double), one (single), or none (negative) of the three immune mediators (IFN-γ, IL-2, and GzmB), are plotted. Results were obtained from two experiments ($n = 3$ to 4 mice per experiment), and a chi-squared test was used to compare the therapeutic versus control arms.

3 billion people currently infected with parasites (79–81), an exploration of inhibitory receptor pathways as targets in parasitic disease (12) or following vaccination warrants further attention. Since studies in the LCMV model have shown the usefulness of combining checkpoint blockade with vaccination to maximize protective immunity (82), and because anti-PD-L1 therapy prevents recrudescence during chronic *T. gondii* infection (13), we explored whether checkpoint blockade could cure virulent secondary infections with *T. gondii*.

Our data suggest that both CD4 and CD8 T cells express receptors associated with T cell exhaustion following challenge with virulent *T. gondii* strains and that CD8 T cells

are hyporesponsive in this context. However, the individual impact of each of these T cell lineages and coreceptors that regulate immunity to reinfection with *T. gondii* is not yet resolved and has likely contributed to our inability to reverse disease outcomes. CD4 T cell help to activate naive CD8 T cells conventionally occurs through CD40-CD40L interactions on both antigen-presenting cells (APCs) (83) and CD40-expressing CD8 T cells (84). CD4 T cell help during primary infection is required to generate memory CD8 T cells that protect against *T. gondii* reinfection (85, 86). During prolonged antigen stimulation, memory CD8 T cells are more reliant on CD4 T cell help than are naive cells to control persistent LCMV infections (87), and CD40-CD40L interactions are likely involved (62). Work by Bhadra et al. suggests that the CD40-CD40L pathway plays a fundamental role in the rescue of exhausted CD8 T cells during chronic *T. gondii* infection (88). For example, following treatment with anti-PD-L1, CD40 was highly expressed on CD8 T cells, and CD8 T cell-intrinsic CD40 signaling played a major role in reinvigorating CD8 T cells during therapy (88). Moreover, the deletion of BLIMP-1 from CD4 T cells restored not only CD4 T cell function but also CD8 T cell function and control of *T. gondii* chronic infection (45). CD4 T cells may also be important in this system. Although CD4 T cells were not impaired in their ability to make IFN-γ, exhaustion markers were expressed on CD4 T cells following virulent secondary infections. Whether CD4 T cell helper functions fail to be propagated in this model of *T. gondii* reinfection is unknown. Further studies could be conducted to assess the role of CD40-CD40L signaling, other costimulatory pathways, and, more generally, CD4 T cell help during secondary challenge with virulent *T. gondii* strains. Costimulatory receptor agonists that mimic helper functions of CD4 T cells might be an avenue for therapeutic intervention in this system.

While PD-1 and TIM-3 were highly expressed on CD4 and CD8 T cells following virulent challenge with *T. gondii*, mice were refractory to therapeutics that target these inhibitory receptors. Previous studies in viral infection models have demonstrated that the state of progression of T cell exhaustion matters during rescue, and perhaps T cells are too exhausted to be rescued following virulent *T. gondii* infections. Exhausted T cells that are T-bet^{hi} and PD-1^{int} are more inclined to be rescued by inhibitory receptor blockade, while exhausted T cells that are EOMES^{hi} and PD-1^{hi} are more prone to die following blockade (17, 89). Furthermore, in mice chronically infected with LCMV, anti-PD-L1 therapy expanded a restricted population of exhausted CD8 T cells, defined by the expression of CXCR5, with properties similar to those of follicular helper T cells (90). Whether a therapeutically responsive population of exhausted T cells is present during *T. gondii* reinfection is unknown. Regardless, anti-CTLA-4 treatment, which has broad effects on recently activated T cells as well as memory T cells, did not rescue mice from virulent challenge. Furthermore, anti-PD-L1–anti-CTLA-4 combination therapy, which promotes superior melanoma clearance in mice (91) and heightened hepatitis C virus (HCV)-specific human CD8 T cell responses *in vitro* (92), again failed to rescue mice from secondary infections with virulent strains of *T. gondii*. While we have not explored the therapeutic effect of targeting all known exhaustion markers described for other systems, our data underscore the context-dependent effects of checkpoint blockade strategies on infection models (26). For example, PD-1 deficiency (93) or PD-1–PD-L1 antibody blockade (94, 95) prolongs mouse survival during bacterial sepsis but rapidly exacerbates disease during *Mycobacterium tuberculosis* infection (9, 10). Understanding the trade-off between enhanced resistance and immune pathology, as well as knowing the pathogen-specific mechanisms required for microbial killing, will be key for predicting the success of immunotherapeutic interventions for infectious disease.

Finally, while memory CD8 T cells are necessary for protection and are the only known memory population to adoptively transfer immunity to naive mice against *T. gondii* strains like RH (43, 50), there are likely additional requirements for immunity to more-virulent strains like GT1, MAS, and GUY-DOS. It is known that immunity cannot be achieved in B cell-deficient mice (96), suggesting a potential role for B cells and/or antibody production in resistance to highly virulent *T. gondii* strains. In summary, although the exhausted T cell phenotype correlates with increased parasite virulence,

this likely represents an effect secondary to an underlying susceptibility factor present in C57BL/6 mice. Identifying this and additional requirements for host immunity to virulent strains of *T. gondii* is the subject of ongoing investigation.

MATERIALS AND METHODS

Parasite strains and cells. Human foreskin fibroblast (HFF) monolayers were grown at 37°C with 5% CO_2 in T-25 flasks for parasite passaging in HFF medium (Dulbecco's modified Eagle's medium [DMEM; Life Technologies] supplemented with 2 mM L-glutamine, 10% fetal bovine serum [FBS; Omega Scientific], 1% penicillin-streptomycin [Life Technologies], and 0.2% gentamicin [Life Technologies]). *Toxoplasma gondii* strains were passaged in HFFs in Toxo medium (4.5 g/liter D-glucose and L-glutamine in DMEM supplemented with 1% FBS and 1% penicillin-streptomycin). The following clonal strains were used (clonal types are indicated in parentheses): RH Δ*hxgprt* (type I), RH Δ*hxgprt* Δ*ku80* (type I), RH *GFP-cLUC* (1-1) (type I), GT1 (type I), Pru (A7) *GFP-fLUC* Δ*hxgprt*::*HXGPRT* (5-8B$^+$) (type II), and CEP *hxgprt*$^-$ (type III). The following atypical strains were used: MAS, MAS *GFP-cLUC* (2C8), and GUY-DOS.

Mice and ethics statements. Six- to seven-week-old female C57BL/6J mice were purchased from Jackson Laboratory. For some experiments, CD45.1 congenic male and female C57BL/6 mice were used. Mouse work was performed in accordance with the National Institutes of Health *Guide for the Care and Use of Laboratory Animals* (97). All protocols were reviewed and approved by the UC Merced Institutional Animal Care and Use Committee. UC Merced has an Animal Welfare Assurance filed with OLAW (assurance number A4561-01), is registered with the USDA (registration number 93-R-0518), and the UC Merced Animal Care Program is AAALAC accredited (accreditation number 001318).

Primary infection and serotyping. Parasite injections were prepared by scraping T-25 flasks containing vacuolated HFFs and sequential syringe lysis first through a 25-gauge needed and then through a 27-gauge needle. The parasites were spun at 400 rpm for 5 min, and the supernatant was transferred, followed by a spin at 1,700 rpm for 7 min. The parasites were washed with 10 ml phosphate-buffered saline (PBS), spun at 1,700 rpm for 7 min, and suspended in PBS. For chronic infections, mice were infected intraperitoneally (i.p.) with 10^4 CEP *hxgprt*$^-$ tachyzoites in 200 μl PBS. Parasite viability in the inoculum was determined by a plaque assay following i.p. infections. A total of 100 or 300 tachyzoites were plated in HFF monolayers grown in a 24-well plate, and 4 to 6 days later, plaques were counted by microscopy (4× objective).

At 30 to 35 days of chronic infection, 50 μl of blood was harvested from mice from the tail vein, collected in tubes containing 5 μl 0.5 M EDTA, and placed on ice. The blood was pelleted at 10,000 rpm for 5 min, and blood plasma was collected from the supernatant and stored at −80°C. To evaluate the seropositivity of the mice, HFFs were grown on coverslips and infected with green fluorescent protein (GFP)-expressing Pru (A7) or RH (1-1) overnight; 18 h later, cells were fixed with 3% formaldehyde in PBS, permeabilized with 3% bovine serum albumin–0.2 M Triton X-100–0.01% sodium azide, incubated with a 1:100 dilution of collected blood plasma for 2 h at room temperature, washed with PBS, and detected with Alexa Fluor 594-labeled secondary antibodies specific for mouse IgG (Life Technologies). Seropositive parasites were observed by immunofluorescence microscopy.

Secondary infections and bioluminescence imaging. Seropositive mice were challenged with 5×10^4 syringe-lysed parasites and euthanized on day 5 for most fluorescence-activated cell sorter (FACS) experiments or weighed every 3 to 4 days for survival experiments. Parasite viability for each strain was determined by a plaque assay following the completion of injections. The viability of the parasites ranged from 20% to 40% of the intended dose. *In vivo* bioluminescence imaging was performed on mice undergoing secondary infection with luciferase-expressing parasites as described previously (52).

Cell isolation, flow cytometry, and *in vitro* recall infections. To isolate peritoneal exudate cells (PECs) by peritoneal lavage, 4 ml of PBS and 3 ml of air were injected into the peritoneal cavity with a 27-gauge needle. After shaking, the puncture was expanded with scissors, and the PEC wash was poured into a conical tube. PEC washes were filtered through a 70-μm cell strainer, pelleted, and washed with FACS buffer (PBS with 1% FBS) before staining. Spleens were dissected, crushed through 70-μm cell strainers, pelleted, suspended in ammonium chloride-potassium (ACK) red blood cell (RBC) lysis buffer for 5 min, quenched with medium containing 10% FBS, and washed with FACS buffer before staining.

For flow cytometry (flow) analysis, cells were further washed in FACS buffer prior to staining. All preparations were done on ice, and cells were blocked in FACS buffer containing Fc block anti-CD16/32 (2.4G2; BD Biosciences), 5% normal hamster serum, and 5% normal rat serum (Jackson ImmunoResearch) prior to staining with fluorophore-conjugated monoclonal antibodies (MAbs). The following MAbs (1:100 staining dilutions) were purchased from eBioscience (Thermo Fisher Scientific) unless otherwise stated: anti-CD4-phycoerythrin (PE)-Cy7 (GK1.5); anti-CD4-fluorescein isothiocyanate (FITC) (clone RM4-5); anti-CD8α-FITC, -allophycocyanin (APC), or -BV510 (53-6.7); anti-CD3ε-eFluor 780 (17A2); anti-CD62L-eFluor 450 (MEL-14); anti-KLRG1-FITC (2F1); anti-PD-1–PE or –APC (J43); anti-TIM-3–PE (RMT3-23); anti-4-1bb (CD137)–PE (17B5); anti-CD25-APC (PC61.5); and anti-CD19-peridinin chlorophyll protein (PerCP)/Cy5.5 (ebio1D3). All nonfixed samples were stained with propidium iodide (PI) (Sigma) at a final concentration of 1 μg/ml. PI-positive (PI$^+$) and CD19$^+$ cells were excluded from the analysis.

For cell enumeration, PBS used for peritoneal lavage was spiked with 5×10^4 BD Calibrite APC beads (BD Bioscience). Beads were identified by FACS analysis as side-scatter high (SSCA^{hi}), PI negative (PI^{neg}), and APC$^+$. The fraction of recovered beads was calculated by taking the count of identified beads and dividing this value by the initial quantity of 5×10^4 beads. Cell enumeration was done by taking the counts of cell populations determined by FACS analysis and dividing them by the fraction of recovered beads per sample.

For the intracellular detection of CTLA-4, cells stained for the surface proteins CD19, CD3ε, CD62L, KLRG1, CD4, CD8α, and PD-1 were then fixed with BD Cytofix/Cytoperm and permeabilized with BD Perm/Wash solution (BD Pharmingen) according to the manufacturer's suggestions. Cells were stained with anti-CTLA-4 (CD152)–PE (UC10-4F10-11) (BD Biosciences) in Perm/Wash solution overnight, washed once with BD Perm/Wash solution and once in FACS buffer, and then analyzed by flow analysis. For the detection of FOXP3, cells were stained for surface proteins CD25, CD3ε, CD4, and CD19 and fixed by using a FoxP3/transcription factor fixation/permeabilization kit (eBioscience) for 45 min at room temperature. Fixed cells were washed and incubated in 1× permeabilization buffer for 10 min prior to intracellular staining with FOXP3-FITC (MF-14; eBioscience) and CTLA-4–PE (UC10-4F10-11) in 1× permeabilization buffer for 45 min and washed once with permeabilization buffer and once with FACS buffer prior to flow analysis.

For *in vitro* recall experiments, splenocytes and PECs were washed and plated in T cell medium (10% FBS in RPMI 1640 with GlutaMAX, antibiotics, 10 mM HEPES, 1 mM sodium pyruvate [Life Technologies], and 1.75 μl β-mercaptoethanol per 500 ml [MP Biomedicals]) at a concentration of 6×10^5 cells per well (96-well plate). Cells were infected with the type I RH, MAS, or GUY-DOS strain at an MOI (multiplicity of infection) of 0.2 for 18 h, and 3 μg/ml brefeldin A (eBioscience) was added for the last 5 h of infection. Ninety-six-well plates were placed on ice, and cells were harvested by pipetting, washed with FACS buffer, blocked, and stained for the surface markers CD4, CD8α, CD3ε, and CD19. Next, cells were fixed with BD Cytofix/Cytoperm and permeabilized with BD Perm/Wash solution (BD Pharmingen) according to the manufacturer's suggestions. Cells were then stained with anti-IFN-γ–PE (XMG1.2), -granzyme B-FITC (GB11), and -IL-2–APC (JES6-5H4) on ice for 1 h or overnight for some experiments. Cells were then washed once with BD Perm/Wash solution and once in FACS buffer and analyzed by FACS. All data were acquired on an LSRII flow cytometer and analyzed with FlowJo software (TreeStar) to compensate and generate flow plots.

Neutralization and T cell depletions. Mice were injected i.p. with 200 μg of the blocking antibodies anti-PD-L1 (10F.9G2), anti-TIM-3 (RMT3-23), and anti-CTLA-4 (9H10) or the rat IgG2b anti-keyhole limpet hemocyanin (KLH) (LTF-2) isotype control antibody, all of which were purchased from BioXCell, on days 1, 3, 5, 7, 10, and 13 after challenge with either the MAS or GT1 strain. Antibody injections were prepared in 200 μl of sterile PBS. Mouse survival and weight were monitored for 27 days. For T cell depletions, chronically infected mice were treated with 400 μg i.p. of anti-CD4 (GK1.5) or anti-CD8a (clone 2.43) on days -7 and -3, before challenge, and on days 3, 7, and 11 after challenge. The efficacy of depletion was determined by flow analysis of peripheral blood lymphocytes (PBLs) on days -1 and 8 of challenge. In brief, 15 μl of whole blood was collected and washed, and red blood cells were lysed with ACK lysis buffer, washed with FACS buffer, blocked, and stained with CD4-FITC (clone RM4-5) and CD8a-APC (clone 53.6-7), as described above. CD4 T cell depletion was determined to be 99.9% and 99.3% effective while CD8 T cell depletion was determined to be 99.7% and 99.5% effective on days -1 and 8, respectively (not shown).

Statistics. One-way analysis of variance (ANOVA) was used to calculate significant differences between means of groups, a log rank (Mantel-Cox) test was used to assess differences in mouse survival between therapeutic treatment and control arms, and a chi-squared test was used to test categorical differences in T cell responses between therapeutic treatment and control arms. Statistics were calculated by using GraphPad Prism software, and a P value of <0.05 was considered significant.

ACKNOWLEDGMENTS

We thank Jeroen Saeij (UC Davis) for initial support of this project and helpful advice and David Gravano (UC Merced) for support with flow analysis. We thank Angel Kongsomboonvech for generating the schematic in Fig. 1.

K.D.C.J. is supported by a Hellman fellowship (Hellman's fund) and the NIH (R15AI131027). The funders had no role in study design, data collection and interpretation, or the decision to submit the work for publication.

S.D.S., S.P.S., and K.D.C.J. conceptualized and designed experiments. S.D.S., S.P.S., K.M.V., K.K.H., and K.D.C.J. analyzed experiments. S.D.S., S.P.S., K.M.V., B.E.C., A.B.C., and K.D.C.J. performed experiments. S.D.S., S.P.S., and K.D.C.J. wrote the manuscript.

REFERENCES

1. Wherry EJ. 2011. T cell exhaustion. Nat Immunol 12:492–499. https://doi.org/10.1038/ni.2035.
2. Zajac AJ, Blattman JN, Murali-Krishna K, Sourdive DJ, Suresh M, Altman JD, Ahmed R. 1998. Viral immune evasion due to persistence of activated T cells without effector function. J Exp Med 188:2205–2213. https://doi.org/10.1084/jem.188.12.2205.
3. Ahmed R, Salmi A, Butler LD, Chiller JM, Oldstone MB. 1984. Selection of genetic variants of lymphocytic choriomeningitis virus in spleens of persistently infected mice. Role in suppression of cytotoxic T lymphocyte response and viral persistence. J Exp Med 160:521–540. https://doi.org/10.1084/jem.160.2.521.
4. Wherry EJ, Blattman JN, Murali-Krishna K, van der Most R, Ahmed R. 2003. Viral persistence alters CD8 T-cell immunodominance and tissue distribution and results in distinct stages of functional impairment. J Virol 77:4911–4927. https://doi.org/10.1128/JVI.77.8.4911-4927.2003.
5. Iwai Y, Ishida M, Tanaka Y, Okazaki T, Honjo T, Minato N. 2002. Involvement of PD-L1 on tumor cells in the escape from host immune system and tumor immunotherapy by PD-L1 blockade. Proc Natl Acad Sci U S A 99:12293–12297. https://doi.org/10.1073/pnas.192461099.
6. Hirano F, Kaneko K, Tamura H, Dong H, Wang S, Ichikawa M, Rietz C, Flies DB, Lau JS, Zhu G, Tamada K, Chen L. 2005. Blockade of B7-H1 and PD-1

by monoclonal antibodies potentiates cancer therapeutic immunity. Cancer Res 65:1089–1096.
7. Sakuishi K, Apetoh L, Sullivan JM, Blazar BR, Kuchroo VK, Anderson AC. 2010. Targeting Tim-3 and PD-1 pathways to reverse T cell exhaustion and restore anti-tumor immunity. J Exp Med 207:2187–2194. https://doi.org/10.1084/jem.20100643.
8. Pauken KE, Wherry EJ. 2015. Overcoming T cell exhaustion in infection and cancer. Trends Immunol 36:265–276. https://doi.org/10.1016/j.it.2015.02.008.
9. Lazar-Molnar E, Chen B, Sweeney KA, Wang EJ, Liu W, Lin J, Porcelli SA, Almo SC, Nathenson SG, Jacobs WR, Jr. 2010. Programmed death-1 (PD-1)-deficient mice are extraordinarily sensitive to tuberculosis. Proc Natl Acad Sci U S A 107:13402–13407. https://doi.org/10.1073/pnas.1007394107.
10. Barber DL, Mayer-Barber KD, Feng CG, Sharpe AH, Sher A. 2011. CD4 T cells promote rather than control tuberculosis in the absence of PD-1-mediated inhibition. J Immunol 186:1598–1607. https://doi.org/10.4049/jimmunol.1003304.
11. Joshi T, Rodriguez S, Perovic V, Cockburn IA, Stager S. 2009. B7-H1 blockade increases survival of dysfunctional CD8(+) T cells and confers protection against Leishmania donovani infections. PLoS Pathog 5:e1000431. https://doi.org/10.1371/journal.ppat.1000431.
12. Butler NS, Moebius J, Pewe LL, Traore B, Doumbo OK, Tygrett LT, Waldschmidt TJ, Crompton PD, Harty JT. 2011. Therapeutic blockade of PD-L1 and LAG-3 rapidly clears established blood-stage Plasmodium infection. Nat Immunol 13:188–195. https://doi.org/10.1038/ni.2180.
13. Bhadra R, Gigley JP, Weiss LM, Khan IA. 2011. Control of Toxoplasma reactivation by rescue of dysfunctional CD8$^+$ T-cell response via PD-1-PDL-1 blockade. Proc Natl Acad Sci U S A 108:9196–9201. https://doi.org/10.1073/pnas.1015298108.
14. Wherry EJ, Ha SJ, Kaech SM, Haining WN, Sarkar S, Kalia V, Subramaniam S, Blattman JN, Barber DL, Ahmed R. 2007. Molecular signature of CD8$^+$ T cell exhaustion during chronic viral infection. Immunity 27:670–684. https://doi.org/10.1016/j.immuni.2007.09.006.
15. Doering TA, Crawford A, Angelosanto JM, Paley MA, Ziegler CG, Wherry EJ. 2012. Network analysis reveals centrally connected genes and pathways involved in CD8$^+$ T cell exhaustion versus memory. Immunity 37:1130–1144. https://doi.org/10.1016/j.immuni.2012.08.021.
16. Crawford A, Angelosanto JM, Kao C, Doering TA, Odorizzi PM, Barnett BE, Wherry EJ. 2014. Molecular and transcriptional basis of CD4(+) T cell dysfunction during chronic infection. Immunity 40:289–302. https://doi.org/10.1016/j.immuni.2014.01.005.
17. Wherry EJ, Kurachi M. 2015. Molecular and cellular insights into T cell exhaustion. Nat Rev Immunol 15:486–499. https://doi.org/10.1038/nri3862.
18. Pauken KE, Sammons MA, Odorizzi PM, Manne S, Godec J, Khan O, Drake AM, Chen Z, Sen DR, Kurachi M, Barnitz RA, Bartman C, Bengsch B, Huang AC, Schenkel JM, Vahedi G, Haining WN, Berger SL, Wherry EJ. 2016. Epigenetic stability of exhausted T cells limits durability of reinvigoration by PD-1 blockade. Science 354:1160–1165. https://doi.org/10.1126/science.aaf2807.
19. Sen DR, Kaminski J, Barnitz RA, Kurachi M, Gerdemann U, Yates KB, Tsao HW, Godec J, LaFleur MW, Brown FD, Tonnerre P, Chung RT, Tully DC, Allen TM, Frahm N, Lauer GM, Wherry EJ, Yosef N, Haining WN. 2016. The epigenetic landscape of T cell exhaustion. Science 354:1165–1169. https://doi.org/10.1126/science.aae0491.
20. Barber DL, Wherry EJ, Masopust D, Zhu B, Allison JP, Sharpe AH, Freeman GJ, Ahmed R. 2006. Restoring function in exhausted CD8 T cells during chronic viral infection. Nature 439:682–687. https://doi.org/10.1038/nature04444.
21. Leach DR, Krummel MF, Allison JP. 1996. Enhancement of antitumor immunity by CTLA-4 blockade. Science 271:1734–1736. https://doi.org/10.1126/science.271.5256.1734.
22. Phan GQ, Yang JC, Sherry RM, Hwu P, Topalian SL, Schwartzentruber DJ, Restifo NP, Haworth LR, Seipp CA, Freezer LJ, Morton KE, Mavroukakis SA, Duray PH, Steinberg SM, Allison JP, Davis TA, Rosenberg SA. 2003. Cancer regression and autoimmunity induced by cytotoxic T lymphocyte-associated antigen 4 blockade in patients with metastatic melanoma. Proc Natl Acad Sci U S A 100:8372–8377. https://doi.org/10.1073/pnas.1533209100.
23. Hodi FS, O'Day SJ, McDermott DF, Weber RW, Sosman JA, Haanen JB, Gonzalez R, Robert C, Schadendorf D, Hassel JC, Akerley W, van den Eertwegh AJ, Lutzky J, Lorigan P, Vaubel JM, Linette GP, Hogg D, Ottensmeier CH, Lebbe C, Peschel C, Quirt I, Clark JI, Wolchok JD, Weber JS, Tian J, Yellin MJ, Nichol GM, Hoos A, Urba WJ. 2010. Improved survival with ipilimumab in patients with metastatic melanoma. N Engl J Med 363:711–723. https://doi.org/10.1056/NEJMoa1003466.
24. Wolchok JD, Kluger H, Callahan MK, Postow MA, Rizvi NA, Lesokhin AM, Segal NH, Ariyan CE, Gordon RA, Reed K, Burke MM, Caldwell A, Kronenberg SA, Agunwamba BU, Zhang X, Lowy I, Inzunza HD, Feely W, Horak CE, Hong Q, Korman AJ, Wigginton JM, Gupta A, Sznol M. 2013. Nivolumab plus ipilimumab in advanced melanoma. N Engl J Med 369:122–133. https://doi.org/10.1056/NEJMoa1302369.
25. Hodi FS, Chesney J, Pavlick AC, Robert C, Grossmann KF, McDermott DF, Linette GP, Meyer N, Giguere JK, Agarwala SS, Shaheen M, Ernstoff MS, Minor DR, Salama AK, Taylor MH, Ott PA, Horak C, Gagnier P, Jiang J, Wolchok JD, Postow MA. 2016. Combined nivolumab and ipilimumab versus ipilimumab alone in patients with advanced melanoma: 2-year overall survival outcomes in a multicentre, randomised, controlled, phase 2 trial. Lancet Oncol 17:1558–1568. https://doi.org/10.1016/S1470-2045(16)30366-7.
26. Attanasio J, Wherry EJ. 2016. Costimulatory and coinhibitory receptor pathways in infectious disease. Immunity 44:1052–1068. https://doi.org/10.1016/j.immuni.2016.04.022.
27. Rao M, Valentini D, Dodoo E, Zumla A, Maeurer M. 2017. Anti-PD-1/PD-L1 therapy for infectious diseases: learning from the cancer paradigm. Int J Infect Dis 56:221–228. https://doi.org/10.1016/j.ijid.2017.01.028.
28. Lehmann T, Graham DH, Dahl ER, Bahia-Oliveira LM, Gennari SM, Dubey JP. 2004. Variation in the structure of Toxoplasma gondii and the roles of selfing, drift, and epistatic selection in maintaining linkage disequilibria. Infect Genet Evol 4:107–114. https://doi.org/10.1016/j.meegid.2004.01.007.
29. Minot S, Melo MB, Li F, Lu D, Niedelman W, Levine SS, Saeij JP. 2012. Admixture and recombination among Toxoplasma gondii lineages explain global genome diversity. Proc Natl Acad Sci U S A 109:13458–13463. https://doi.org/10.1073/pnas.1117047109.
30. Su C, Khan A, Zhou P, Majumdar D, Ajzenberg D, Dardé M, Zhu X, Ajioka JW, Rosenthal BM, Dubey JP, Sibley LD. 2012. Globally diverse Toxoplasma gondii isolates comprise six major clades originating from a small number of distinct ancestral lineages. Proc Natl Acad Sci U S A 109:5844–5849. https://doi.org/10.1073/pnas.1203190109.
31. Lorenzi H, Khan A, Behnke MS, Namasivayam S, Swapna LS, Hadjithomas M, Karamycheva S, Pinney D, Brunk BP, Ajioka JW, Ajzenberg D, Boothroyd JC, Boyle JP, Darde ML, Diaz-Miranda MA, Dubey JP, Fritz HM, Gennari SM, Gregory BD, Kim K, Saeij JP, Su C, White MW, Zhu XQ, Howe DK, Rosenthal BM, Grigg ME, Parkinson J, Liu L, Kissinger JC, Roos DS, Sibley LD. 2016. Local admixture of amplified and diversified secreted pathogenesis determinants shapes mosaic Toxoplasma gondii genomes. Nat Commun 7:10147. https://doi.org/10.1038/ncomms10147.
32. Howe DK, Sibley LD. 1995. Toxoplasma gondii comprises three clonal lineages: correlation of parasite genotype with human disease. J Infect Dis 172:1561–1566. https://doi.org/10.1093/infdis/172.6.1561.
33. Sibley LD, Boothroyd JC. 1992. Virulent strains of Toxoplasma gondii comprise a single clonal lineage. Nature 359:82–85. https://doi.org/10.1038/359082a0.
34. Su C, Evans D, Cole RH, Kissinger JC, Ajioka JW, Sibley LD. 2003. Recent expansion of Toxoplasma through enhanced oral transmission. Science 299:414–416. https://doi.org/10.1126/science.1078035.
35. Fux B, Nawas J, Khan A, Gill DB, Su C, Sibley LD. 2007. Toxoplasma gondii strains defective in oral transmission are also defective in developmental stage differentiation. Infect Immun 75:2580–2590. https://doi.org/10.1128/IAI.00085-07.
36. Yarovinsky F. 2014. Innate immunity to Toxoplasma gondii infection. Nat Rev Immunol 14:109–121. https://doi.org/10.1038/nri3598.
37. Konradt C, Ueno N, Christian DA, Delong JH, Pritchard GH, Herz J, Bzik DJ, Koshy AA, McGavern DB, Lodoen MB, Hunter CA. 2016. Endothelial cells are a replicative niche for entry of Toxoplasma gondii to the central nervous system. Nat Microbiol 1:16001. https://doi.org/10.1038/nmicrobiol.2016.1.
38. Suzuki Y, Conley FK, Remington JS. 1989. Importance of endogenous IFN-gamma for prevention of toxoplasmic encephalitis in mice. J Immunol 143:2045–2050.
39. Gazzinelli R, Xu Y, Hieny S, Cheever A, Sher A. 1992. Simultaneous depletion of CD4$^+$ and CD8$^+$ T lymphocytes is required to reactivate chronic infection with Toxoplasma gondii. J Immunol 149:175–180.
40. Kang H, Suzuki Y. 2001. Requirement of non-T cells that produce gamma interferon for prevention of reactivation of Toxoplasma gondii infection in the brain. Infect Immun 69:2920–2927. https://doi.org/10.1128/IAI.69.5.2920-2927.2001.

41. Suzuki Y, Wang X, Jortner BS, Payne L, Ni Y, Michie SA, Xu B, Kudo T, Perkins S. 2010. Removal of Toxoplasma gondii cysts from the brain by perforin-mediated activity of CD8$^+$ T cells. Am J Pathol 176:1607–1613. https://doi.org/10.2353/ajpath.2010.090825.
42. Bhadra R, Cobb DA, Khan IA. 2013. Donor CD8$^+$ T cells prevent Toxoplasma gondii de-encystation but fail to rescue the exhausted endogenous CD8$^+$ T cell population. Infect Immun 81:3414–3425. https://doi.org/10.1128/IAI.00784-12.
43. Gigley JP, Bhadra R, Khan IA. 2011. CD8 T cells and Toxoplasma gondii: a new paradigm. J Parasitol Res 2011:243796. https://doi.org/10.1155/2011/243796.
44. Bhadra R, Gigley JP, Khan IA. 2012. PD-1-mediated attrition of polyfunctional memory CD8$^+$ T cells in chronic toxoplasma infection. J Infect Dis 206:125–134. https://doi.org/10.1093/infdis/jis304.
45. Hwang S, Cobb DA, Bhadra R, Youngblood B, Khan IA. 2016. Blimp-1-mediated CD4 T cell exhaustion causes CD8 T cell dysfunction during chronic toxoplasmosis. J Exp Med 213:1799–1818. https://doi.org/10.1084/jem.20151995.
46. Murphy ML, Cotterell SE, Gorak PM, Engwerda CR, Kaye PM. 1998. Blockade of CTLA-4 enhances host resistance to the intracellular pathogen, Leishmania donovani. J Immunol 161:4153–4160.
47. McCoy K, Camberis M, Gros GL. 1997. Protective immunity to nematode infection is induced by CTLA-4 blockade. J Exp Med 186:183–187. https://doi.org/10.1084/jem.186.2.183.
48. Gazzinelli RT, Hakim FT, Hieny S, Shearer GM, Sher A. 1991. Synergistic role of CD4$^+$ and CD8$^+$ T lymphocytes in IFN-gamma production and protective immunity induced by an attenuated Toxoplasma gondii vaccine. J Immunol 146:286–292.
49. Jordan KA, Wilson EH, Tait ED, Fox BA, Roos DS, Bzik DJ, Dzierszinski F, Hunter CA. 2009. Kinetics and phenotype of vaccine-induced CD8$^+$ T-cell responses to Toxoplasma gondii. Infect Immun 77:3894–3901. https://doi.org/10.1128/IAI.00024-09.
50. Gigley JP, Fox BA, Bzik DJ. 2009. Cell-mediated immunity to Toxoplasma gondii develops primarily by local Th1 host immune responses in the absence of parasite replication. J Immunol 182:1069–1078. https://doi.org/10.4049/jimmunol.182.2.1069.
51. Fox BA, Bzik DJ. 2002. De novo pyrimidine biosynthesis is required for virulence of Toxoplasma gondii. Nature 415:926–929. https://doi.org/10.1038/415926a.
52. Jensen KD, Camejo A, Melo MB, Cordeiro C, Julien L, Grotenbreg GM, Frickel EM, Ploegh HL, Young L, Saeij JP. 2015. Toxoplasma gondii superinfection and virulence during secondary infection correlate with the exact ROP5/ROP18 allelic combination. mBio 6:e02280-14. https://doi.org/10.1128/mBio.02280-14.
53. Suzuki Y, Remington JS. 1988. Dual regulation of resistance against Toxoplasma gondii infection by Lyt-2$^+$ and Lyt-1$^+$, L3T4$^+$ T cells in mice. J Immunol 140:3943–3946.
54. Suzuki Y, Sa Q, Gehman M, Ochiai E. 2011. Interferon-gamma- and perforin-mediated immune responses for resistance against Toxoplasma gondii in the brain. Expert Rev Mol Med 13:e31. https://doi.org/10.1017/S1462399411002018.
55. Ochiai E, Sa Q, Perkins S, Grigg ME, Suzuki Y. 2016. CD8(+) T cells remove cysts of Toxoplasma gondii from the brain mostly by recognizing epitopes commonly expressed by or cross-reactive between type II and type III strains of the parasite. Microbes Infect 18:517–522. https://doi.org/10.1016/j.micinf.2016.03.013.
56. Masopust D, Schenkel JM. 2013. The integration of T cell migration, differentiation and function. Nat Rev Immunol 13:309–320. https://doi.org/10.1038/nri3442.
57. Sallusto F, Geginat J, Lanzavecchia A. 2004. Central memory and effector memory T cell subsets: function, generation, and maintenance. Annu Rev Immunol 22:745–763. https://doi.org/10.1146/annurev.immunol.22.012703.104702.
58. Robbins SH, Terrizzi SC, Sydora BC, Mikayama T, Brossay L. 2003. Differential regulation of killer cell lectin-like receptor G1 expression on T cells. J Immunol 170:5876–5885. https://doi.org/10.4049/jimmunol.170.12.5876.
59. Wilson DC, Grotenbreg GM, Liu K, Zhao Y, Frickel EM, Gubbels MJ, Ploegh HL, Yap GS. 2010. Differential regulation of effector- and central-memory responses to Toxoplasma gondii infection by IL-12 revealed by tracking of Tgd057-specific CD8$^+$ T cells. PLoS Pathog 6:e1000815. https://doi.org/10.1371/journal.ppat.1000815.
60. Chu HH, Chan SW, Gosling JP, Blanchard N, Tsitsiklis A, Lythe G, Shastri N, Molina-Paris C, Robey EA. 2016. Continuous effector CD8(+) T cell production in a controlled persistent infection is sustained by a proliferative intermediate population. Immunity 45:159–171. https://doi.org/10.1016/j.immuni.2016.06.013.
61. Wilson DC, Matthews S, Yap GS. 2008. IL-12 signaling drives CD8$^+$ T cell IFN-gamma production and differentiation of KLRG1$^+$ effector subpopulations during Toxoplasma gondii infection. J Immunol 180:5935–5945. https://doi.org/10.4049/jimmunol.180.9.5935.
62. West EE, Youngblood B, Tan WG, Jin HT, Araki K, Alexe G, Konieczny BT, Calpe S, Freeman GJ, Terhorst C, Haining WN, Ahmed R. 2011. Tight regulation of memory CD8(+) T cells limits their effectiveness during sustained high viral load. Immunity 35:285–298. https://doi.org/10.1016/j.immuni.2011.05.017.
63. Alegre ML, Noel PJ, Eisfelder BJ, Chuang E, Clark MR, Reiner SL, Thompson CB. 1996. Regulation of surface and intracellular expression of CTLA4 on mouse T cells. J Immunol 157:4762–4770.
64. Blackburn SD, Shin H, Haining WN, Zou T, Workman CJ, Polley A, Betts MR, Freeman GJ, Vignali DA, Wherry EJ. 2009. Coregulation of CD8$^+$ T cell exhaustion by multiple inhibitory receptors during chronic viral infection. Nat Immunol 10:29–37. https://doi.org/10.1038/ni.1679.
65. Egen JG, Kuhns MS, Allison JP. 2002. CTLA-4: new insights into its biological function and use in tumor immunotherapy. Nat Immunol 3:611–618. https://doi.org/10.1038/ni0702-611.
66. Jin HT, Anderson AC, Tan WG, West EE, Ha SJ, Araki K, Freeman GJ, Kuchroo VK, Ahmed R. 2010. Cooperation of Tim-3 and PD-1 in CD8 T-cell exhaustion during chronic viral infection. Proc Natl Acad Sci U S A 107:14733–14738. https://doi.org/10.1073/pnas.1009731107.
67. Krummel MF, Allison JP. 1995. CD28 and CTLA-4 have opposing effects on the response of T cells to stimulation. J Exp Med 182:459–465. https://doi.org/10.1084/jem.182.2.459.
68. Krummel MF, Allison JP. 1996. CTLA-4 engagement inhibits IL-2 accumulation and cell cycle progression upon activation of resting T cells. J Exp Med 183:2533–2540. https://doi.org/10.1084/jem.183.6.2533.
69. Parry RV, Chemnitz JM, Frauwirth KA, Lanfranco AR, Braunstein I, Kobayashi SV, Linsley PS, Thompson CB, Riley JL. 2005. CTLA-4 and PD-1 receptors inhibit T-cell activation by distinct mechanisms. Mol Cell Biol 25:9543–9553. https://doi.org/10.1128/MCB.25.21.9543-9553.2005.
70. Liakou CI, Kamat A, Tang DN, Chen H, Sun J, Troncoso P, Logothetis C, Sharma P. 2008. CTLA-4 blockade increases IFNgamma-producing CD4$^+$ ICOS^{hi} cells to shift the ratio of effector to regulatory T cells in cancer patients. Proc Natl Acad Sci U S A 105:14987–14992. https://doi.org/10.1073/pnas.0806075105.
71. Kalia V, Penny LA, Yuzefpolskiy Y, Baumann FM, Sarkar S. 2015. Quiescence of memory CD8(+) T cells is mediated by regulatory T cells through inhibitory receptor CTLA-4. Immunity 42:1116–1129. https://doi.org/10.1016/j.immuni.2015.05.023.
72. Chambers CA, Sullivan TJ, Truong T, Allison JP. 1998. Secondary but not primary T cell responses are enhanced in CTLA-4-deficient CD8$^+$ T cells. Eur J Immunol 28:3137–3143. https://doi.org/10.1002/(SICI)1521-4141(199810)28:10<3137::AID-IMMU3137>3.0.CO;2-X.
73. Minn AJ, Wherry EJ. 2016. Combination cancer therapies with immune checkpoint blockade: convergence on interferon signaling. Cell 165:272–275. https://doi.org/10.1016/j.cell.2016.03.031.
74. Benci JL, Xu B, Qiu Y, Wu TJ, Dada H, Twyman-Saint Victor C, Cucolo L, Lee DSM, Pauken KE, Huang AC, Gangadhar TC, Amaravadi RK, Schuchter LM, Feldman MD, Ishwaran H, Vonderheide RH, Maity A, Wherry EJ, Minn AJ. 2016. Tumor interferon signaling regulates a multigenic resistance program to immune checkpoint blockade. Cell 167:1540.e12–1554.e12. https://doi.org/10.1016/j.cell.2016.11.022.
75. RTS,S Clinical Trials Partnership. 2015. Efficacy and safety of RTS,S/AS01 malaria vaccine with or without a booster dose in infants and children in Africa: final results of a phase 3, individually randomised, controlled trial. Lancet 386:31–45. https://doi.org/10.1016/S0140-6736(15)60721-8.
76. Siegrist C. 2008. Vaccine immunology, p 17–36. *In* Plotkin SA, Orenstein W, Offit P (ed), Vaccines, 5th ed. Elsevier Inc, Philadelphia, PA.
77. Sacks DL. 2014. Vaccines against tropical parasitic diseases: a persisting answer to a persisting problem. Nat Immunol 15:403–405. https://doi.org/10.1038/ni.2853.
78. Sher A, Coffman RL. 1992. Regulation of immunity to parasites by T cells and T cell-derived cytokines. Annu Rev Immunol 10:385–409. https://doi.org/10.1146/annurev.iy.10.040192.002125.
79. Hotez PJ, Alvarado M, Basanez MG, Bolliger I, Bourne R, Boussinesq M, Brooker SJ, Brown AS, Buckle G, Budke CM, Carabin H, Coffeng LE, Fevre EM, Furst T, Halasa YA, Jasrasaria R, Johns NE, Keiser J, King CH, Lozano R, Murdoch ME, O'Hanlon S, Pion SD, Pullan RL, Ramaiah KD, Roberts T, Shepard DS, Smith JL, Stolk WA, Undurraga EA, Utzinger J, Wang M,

Murray CJ, Naghavi M. 2014. The global burden of disease study 2010: interpretation and implications for the neglected tropical diseases. PLoS Negl Trop Dis 8:e2865. https://doi.org/10.1371/journal.pntd.0002865.
80. Torgerson PR, de Silva NR, Fevre EM, Kasuga F, Rokni MB, Zhou XN, Sripa B, Gargouri N, Willingham AL, Stein C. 2014. The global burden of foodborne parasitic diseases: an update. Trends Parasitol 30:20–26. https://doi.org/10.1016/j.pt.2013.11.002.
81. Pullan RL, Smith JL, Jasrasaria R, Brooker SJ. 2014. Global numbers of infection and disease burden of soil transmitted helminth infections in 2010. Parasit Vectors 7:37. https://doi.org/10.1186/1756-3305-7-37.
82. Ha SJ, Mueller SN, Wherry EJ, Barber DL, Aubert RD, Sharpe AH, Freeman GJ, Ahmed R. 2008. Enhancing therapeutic vaccination by blocking PD-1-mediated inhibitory signals during chronic infection. J Exp Med 205:543–555. https://doi.org/10.1084/jem.20071949.
83. Schoenberger SP, Toes RE, van der Voort EI, Offringa R, Melief CJ. 1998. T-cell help for cytotoxic T lymphocytes is mediated by CD40-CD40L interactions. Nature 393:480–483. https://doi.org/10.1038/31002.
84. Bourgeois C, Rocha B, Tanchot C. 2002. A role for CD40 expression on $CD8^+$ T cells in the generation of $CD8^+$ T cell memory. Science 297:2060–2063. https://doi.org/10.1126/science.1072615.
85. Denkers EY, Scharton-Kersten T, Barbieri S, Caspar P, Sher A. 1996. A role for $CD4^+$ $NK1.1^+$ T lymphocytes as major histocompatibility complex class II independent helper cells in the generation of $CD8^+$ effector function against intracellular infection. J Exp Med 184:131–139. https://doi.org/10.1084/jem.184.1.131.
86. Casciotti L, Ely KH, Williams ME, Khan IA. 2002. $CD8^+$-T-cell immunity against Toxoplasma gondii can be induced but not maintained in mice lacking conventional $CD4^+$ T cells. Infect Immun 70:434–443. https://doi.org/10.1128/IAI.70.2.434-443.2002.
87. Aubert RD, Kamphorst AO, Sarkar S, Vezys V, Ha SJ, Barber DL, Ye L, Sharpe AH, Freeman GJ, Ahmed R. 2011. Antigen-specific CD4 T-cell help rescues exhausted CD8 T cells during chronic viral infection. Proc Natl Acad Sci U S A 108:21182–21187. https://doi.org/10.1073/pnas.1118450109.
88. Bhadra R, Gigley JP, Khan IA. 2011. Cutting edge: CD40-CD40 ligand pathway plays a critical CD8-intrinsic and -extrinsic role during rescue of exhausted CD8 T cells. J Immunol 187:4421–4425. https://doi.org/10.4049/jimmunol.1102319.
89. Paley MA, Kroy DC, Odorizzi PM, Johnnidis JB, Dolfi DV, Barnett BE, Bikoff EK, Robertson EJ, Lauer GM, Reiner SL, Wherry EJ. 2012. Progenitor and terminal subsets of $CD8^+$ T cells cooperate to contain chronic viral infection. Science 338:1220–1225. https://doi.org/10.1126/science.1229620.
90. Im SJ, Hashimoto M, Gerner MY, Lee J, Kissick HT, Burger MC, Shan Q, Hale JS, Lee J, Nasti TH, Sharpe AH, Freeman GJ, Germain RN, Nakaya HI, Xue HH, Ahmed R. 2016. Defining $CD8^+$ T cells that provide the proliferative burst after PD-1 therapy. Nature 537:417–421. https://doi.org/10.1038/nature19330.
91. Curran MA, Montalvo W, Yagita H, Allison JP. 2010. PD-1 and CTLA-4 combination blockade expands infiltrating T cells and reduces regulatory T and myeloid cells within B16 melanoma tumors. Proc Natl Acad Sci U S A 107:4275–4280. https://doi.org/10.1073/pnas.0915174107.
92. Nakamoto N, Cho H, Shaked A, Olthoff K, Valiga ME, Kaminski M, Gostick E, Price DA, Freeman GJ, Wherry EJ, Chang KM. 2009. Synergistic reversal of intrahepatic HCV-specific CD8 T cell exhaustion by combined PD-1/CTLA-4 blockade. PLoS Pathog 5:e1000313. https://doi.org/10.1371/journal.ppat.1000313.
93. Huang X, Venet F, Wang YL, Lepape A, Yuan Z, Chen Y, Swan R, Kherouf H, Monneret G, Chung CS, Ayala A. 2009. PD-1 expression by macrophages plays a pathologic role in altering microbial clearance and the innate inflammatory response to sepsis. Proc Natl Acad Sci U S A 106:6303–6308. https://doi.org/10.1073/pnas.0809422106.
94. Brahmamdam P, Inoue S, Unsinger J, Chang KC, McDunn JE, Hotchkiss RS. 2010. Delayed administration of anti-PD-1 antibody reverses immune dysfunction and improves survival during sepsis. J Leukoc Biol 88:233–240. https://doi.org/10.1189/jlb.0110037.
95. Zhang Y, Zhou Y, Lou J, Li J, Bo L, Zhu K, Wan X, Deng X, Cai Z. 2010. PD-L1 blockade improves survival in experimental sepsis by inhibiting lymphocyte apoptosis and reversing monocyte dysfunction. Crit Care 14:R220. https://doi.org/10.1186/cc9354.
96. Sayles PC, Gibson GW, Johnson LL. 2000. B cells are essential for vaccination-induced resistance to virulent Toxoplasma gondii. Infect Immun 68:1026–1033. https://doi.org/10.1128/IAI.68.3.1026-1033.2000.
97. National Research Council. 2011. Guide for the care and use of laboratory animals, 8th ed. National Academies Press, Washington, DC.